

Optimal Planning and Control of a Noisy Car-Like Robot with Obstacle Avoidance

Spencer Powers

May 9, 2022



JOHNS HOPKINS
WHITING SCHOOL
of ENGINEERING

Final project for EN.530.678: Nonlinear Control and Planning in Robotics

1 Problem Formulation

This project focused on optimal trajectory generation and robust feedback control for the car-like robot shown in Figure 1. The generalized task is moving between a starting and desired vehicle configuration while avoiding obstacles and exclusion zones.

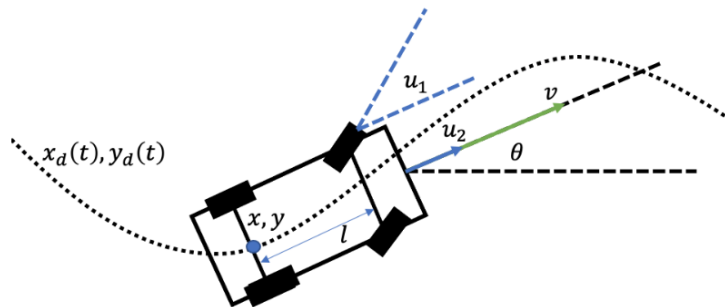


Figure 1: State variables and controls of the vehicle.

The equations of motion for the vehicle are as follows:

$$\begin{bmatrix} \dot{x} \\ \dot{y} \\ \dot{\theta} \\ \dot{v} \end{bmatrix} = \begin{bmatrix} v \cos(\theta) \\ v \sin(\theta) \\ 0 \\ 0 \end{bmatrix} + \begin{bmatrix} 0 & 0 \\ 0 & 0 \\ v/l & 0 \\ 0 & 1 \end{bmatrix} \left(\begin{bmatrix} \tan(u_1) \\ u_2 \end{bmatrix} + \delta(v, K) \right)$$

where (x, y) denotes the position of the center of the rear axle, θ is the heading angle, v is the forward velocity, l is the distance between axles, u_1 is the turning angle, and u_2 is the forward acceleration. The δ term is random control noise where the magnitude of each component is bounded by $|\delta_i| \leq k_i v (1 + K)$ for which k_i is a scaling constant determined by a given noise benchmark and K is the curvature, i.e. $K = \tan(u_1)/l$.

For computing collisions with obstacles and exclusion zones, the car body shape is approximated as two circles of a specified diameter, each centered at the midpoint of one of the axles.

While the primary goal of this project was to generate and robustly track ideal trajectories with a nominal amount of injected control noise, the secondary goal was to test the robustness of the derived control law to varying noise magnitude.

2 Methods

2.1 Optimal Trajectory Generation

The optimal trajectory generation problem can be formulated as finding the optimal control sequence that minimizes the following trajectory cost while sat-

isfying given initial conditions and various constraints, including differential constraints (e.g. the vehicle dynamics) and algebraic constraints (e.g. distance from obstacles):

$$J = \frac{1}{2}q(t_f)^T P_f q(t_f) + \int_{t_0}^{t_f} \frac{1}{2} (q^T Q q + u^T R u) \quad (1)$$

where $q = [xy\theta v]^T$ is the state vector and P_f , Q , and R are penalty coefficient matrices that influence the optimization behavior. Differential dynamic programming (DDP) was used to actually solve the constrained optimization problem and produce the ideal trajectories. Specifically, 50 solver iterations were used, the time horizon was set to 15 seconds, Q was set to 0, and Q_f and R were tuned to produce the desired solver behavior. In addition, the turning angle u_1 was constrained between $[-45, 45]$ degrees and forward acceleration u_2 was constrained between $[-1, 1]$ m/s².

2.2 Control Noise Benchmarks

The noise scaling coefficients k_i were computed using the following benchmarks. For u_1 , a maximum drift of 5° was specified at 60 mph (or 26.8 m/s) and at a desired turning angle of 45°. Since this noise is added to $\tan(u_1)$, k_1 is computed via:

$$k_1 = \frac{\tan(45) - \tan(40)}{26.8 * (1 + \tan(45)/l)}$$

Similarly, for u_2 , a maximum drift of 1 m/s² was specified under the same driving conditions, and thus k_2 is computed via:

$$k_2 = \frac{1}{26.8 * (1 + \tan(45)/l)}$$

2.3 Feedback Control Law Derivation

The control law $u = \psi + \nu$ was derived via backstepping and Lyapunov redesign, where ψ stabilizes the nominal system and ν is a disturbance rejection term to handle the injected control noise. Let $e = h - h_d$, where the output h is $[x, y]$. Let the initial Lyapunov function be $V_0 = \frac{1}{2}e^T e$. Taking the time derivative, this yields:

$$\dot{V}_0 = e^T \dot{e} = e^T (\dot{h} - \dot{h}_d) = e^T \left(\begin{bmatrix} v \cos(\theta) \\ v \sin(\theta) \end{bmatrix} - \dot{h}_d \right)$$

If \dot{h} was controllable, we could choose to set it to $\dot{h}_d - k_1 e$ where $k_1 > 0$ to make $\dot{V}_0 = -k_1 e^T e$, which is negative definite and would thus asymptotically stabilize the error dynamics. However, \dot{h} is not directly controllable, so define a new error $z = \dot{h} - (\dot{h}_d - k_1 e)$. Now define a new Lyapunov function as $V = V_0 + \frac{1}{2}z^T z$. Taking the time derivative and manipulating the terms yields the following:

$$\dot{V} = e^T \dot{e} + z^T \dot{z} = e^T (z - k_1 e) + z^T \dot{z} = -k_1 e^T e + z^T (e + \dot{z})$$

Expanding the \dot{z} term yields:

$$\dot{V} = -k_1 e^T e + z^T (e + R\bar{u} - \ddot{h}_d + k_1 \dot{e})$$

where $R = \begin{bmatrix} -v^2 \sin(\theta)/l & \cos(\theta) \\ v^2 \cos(\theta)/l & \sin(\theta) \end{bmatrix}$ and $\bar{u} = \begin{bmatrix} \tan(u_1) \\ u_2 \end{bmatrix}$.

Finally, we can choose to set \bar{u} to be:

$$\bar{u} = R^{-1} (-e + \ddot{h}_d - k_1 \dot{e} - k_2 z)$$

such that $\dot{V} = -k_1 e^T e - k_2 z^T z$, which is negative definite and would thus asymptotically stabilize both errors around 0. This yields the nominal control law that stabilizes the noise-free system:

$$\psi = \begin{bmatrix} \tan^{-1}(\bar{u}_1) \\ \bar{u}_2 \end{bmatrix}$$

Next, the disturbance rejection term ν is derived via Lyapunov redesign. First, the dynamics can be written in the form $\dot{q} = f(q) + G(q)\bar{u}$. Second, the nominal controller ψ has an associated Lyapunov function V . Third, the noise bound can be expressed as $\|\delta\| \leq \rho(t, q) + k_0 \|\nu\|$, where in this case $\rho(t, q) = k_{tot} v (1 + K)$, $k_{tot} = \|[k_1, k_2]\|$, and $k_0 = 0$.

Let $w = G^T \nabla_q V$. The disturbance rejection term ν can then be computed via:

$$\nu = -\eta(t, q) \frac{w}{\|w\|}$$

where

$$\eta(t, q) \geq \frac{\rho(t, q)}{1 - k_0} = k_{tot} v (1 + K)$$

To resolve chattering issues that arise when the vehicle is close to the ideal trajectory and thus $\|w\|$ approaches 0, a piecewise form of ν is used:

$$\nu = \begin{cases} -\eta(t, q) \frac{w}{\|w\|} & \eta \|w\| \geq \epsilon \\ -\eta^2(t, q) \frac{w}{\epsilon} & \eta \|w\| < \epsilon \end{cases}$$

where ϵ is an arbitrarily small constant that defines the radius of a tube around the ideal trajectory in state space. The controller is only guaranteed to be asymptotically stable towards the ideal trajectory outside of this tube, but it has better numerical stability properties inside of the tube and thus close to the ideal trajectory because it avoids divide-by-zero issues.

This piecewise form of the disturbance rejection term, when combined with the previously-derived nominal controller, yields the final control law $u = \psi + \nu$.

3 Example Scenario

Consider the following example scenario. Let $q_0 = [-6, -4, 0, 0]^T$, $q_d = [5, -1, 0, 0]^T$, $l = 1$, $r_c = 0.5$, $t_f = 15$, $Q_f = 50 * \text{diag}([1, 1, 1, 1])$, and $R = 4 * \text{diag}([1, 1])$. A circular obstacle of radius 1 is centered at $p_o = (1.5, -2.5)$, and an exclusion zone boundary line is defined by $y = 0.3x - 5.5$ that the vehicle must remain above. The real initial starting condition is $q_{0, \text{noisy}} = q_0 + [0.1, 0.1, 0.1, 0.1]^T$. The control constraints and noise benchmarks are described in the previous section.

The optimal trajectory generation starting from the nominal initial condition with noise-free dynamics and the ideal controls associated with the optimal trajectory are shown in Figure 2:

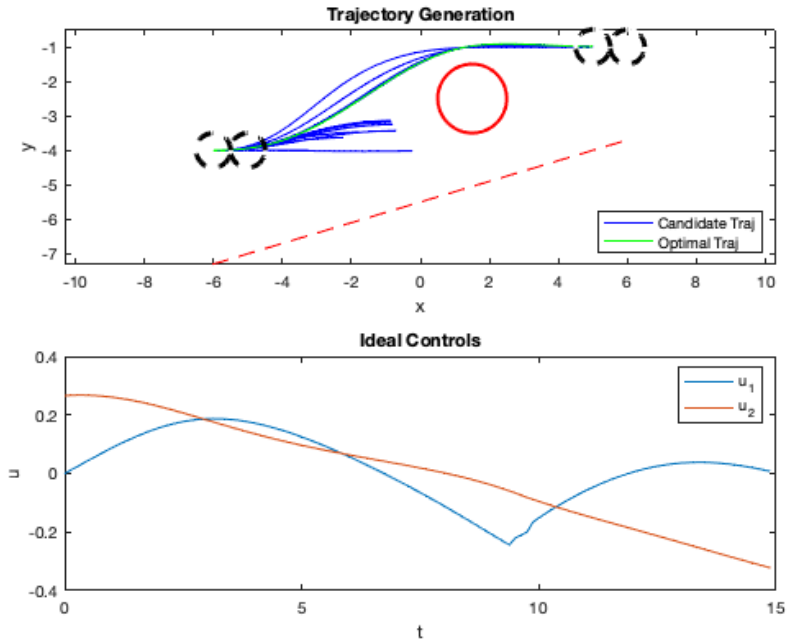


Figure 2: Optimal trajectory generation and associated controls. Dashed circles represent the circles centered on each axle for the collision detection model.

The following figure shows the trajectory tracking process, namely starting at the noisy initial condition and simulating the evolution of the vehicle using the derived feedback control law with injected control noise:

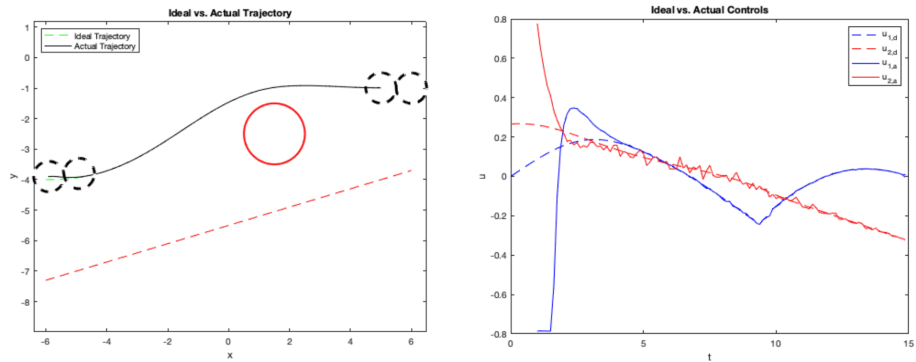


Figure 3: Noisy trajectory tracking using the derived feedback control law. Dashed circles represent the circles centered on each axle for the collision detection model.

The performance of the controller is summarized via the following tracking error plot, and the distance to the nearest obstacle over time is also provided:

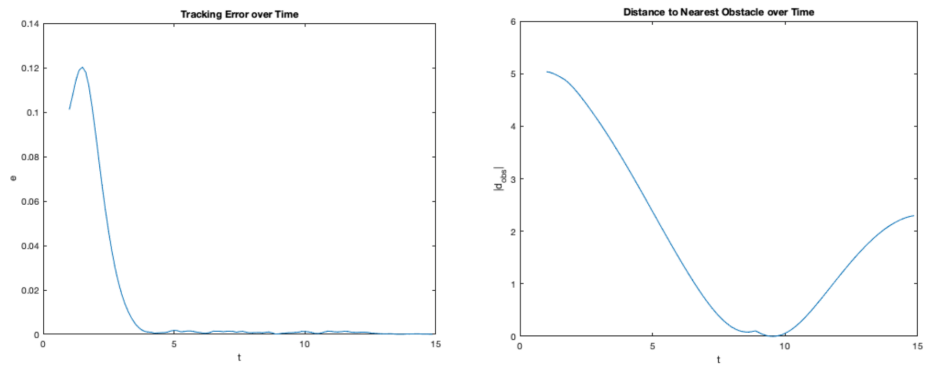


Figure 4: Tracking error and distance to nearest obstacle over time.

To test the robustness of the controller to noise, both noise benchmarks were doubled to 10° and 2 m/s^2 and the tracking performance was re-evaluated. The trajectory tracking and controls are shown in the following figure:

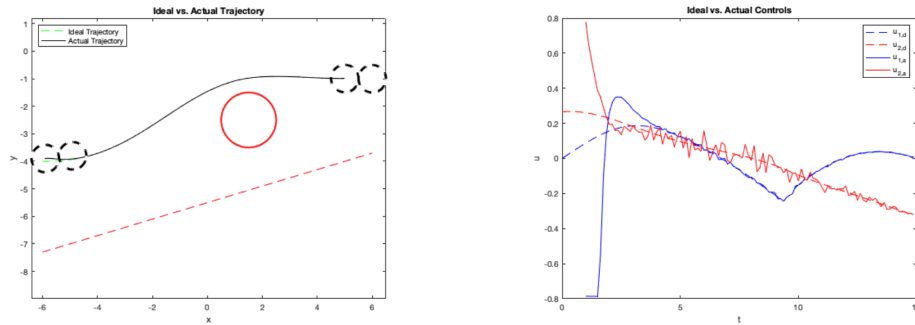


Figure 5: Noisy trajectory tracking using the derived feedback control law with doubled noise benchmarks. Dashed circles represent the circles centered on each axle for the collision detection model.

The resulting actual controls are slightly noisier, but the tracking itself remains exceptionally good. This is also seen quantitatively in the tracking error plot below. The distance to the nearest obstacle is also provided to show that collisions are still avoided over the course of the actual trajectory.

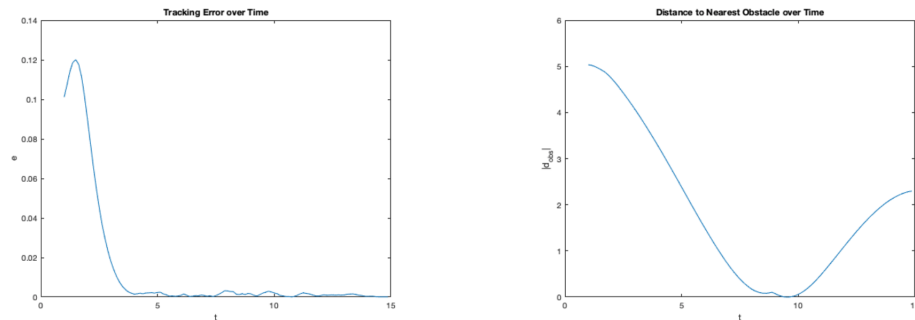


Figure 6: Tracking error and distance to nearest obstacle over time with doubled noise benchmarks.

4 Conclusion

Differential dynamic programming was successfully leveraged to generate optimal trajectories that satisfied given vehicle dynamics and control constraints while avoiding obstacles and exclusion zones. Backstepping and Lyapunov redesign were successfully used to derive a feedback control law that exhibits robustness to bounded control noise that varies as a function of vehicle speed and curvature.